32nd URSI GASS, Montreal, 19–26 August 2017

An Experimental Study of Microwave Remote Sensing of Oil-Contaminated Young Sea Ice

Nariman Firoozy[(1)], Thomas Neusitzer[(2)], Durell Desmond[(1)], Tyler Tiede[(2)], Marcos Lemes[(1)], Jack Landy[(3)], Gary Stern[(1)], Puyan Mojabi[(2)], Søren Rysgaard[(1)], and David G. Barber[(1)]

(1) Centre for Earth Observation Science, University of Manitoba, Winnipeg, Canada

(2) Department of Electrical and Computer Engineering, University of Manitoba, Winnipeg, Canada

(3) School of Geographical Sciences, University of Bristol, Bristol, United Kingdom

Abstract

This paper presents an experiment on remote sensing of oil infested sea ice, and the detection of this contaminant. To this end, an overview of our previously developed electromagnetic inversion algorithm is first presented. This algorithm has been able to reconstruct the complex permittivity profile of snow-covered sea ice, and also retrieve some of its thermodynamic and geophysical properties. Next, a description of our oil-in-sea ice experiment is presented in which crude oil is injected underneath an artificially-grown young sea ice as the resulting radar cross section response is temporally measured. The volume fraction of oil is then indirectly retrieved using the measured radar data via a modified inversion strategy. Although the reconstructed volume fraction is an over-estimation, it has a potential to trigger a warning system. Finally, the reasons behind this overestimation are discussed.

1 Introduction

Arctic sea ice extent has been shrinking in the past few decades, and a summertime ice-free Arctic is predicted to happen before the mid-century, with an estimated two decades uncertainty [1, 2]. Considering the Arctic's harsh environment, sheer size, and remoteness, microwave remote sensing has been the primary choice in observation and quantification of Arctic changes due to its ability in covering large areas during day and night, and being minimally affected by weather conditions. This technology can also be utilized for monitoring and parameter retrieval in areas of increased activities in the Arctic, for instance, the revitalized Northwest Passage shipping route [3].

Remote sensing retrieval models are generally either statistical (*i.e.*, developed based on previous measurements and their associated observed parameters), or physical-based (*i.e.*, reliant on the simulation of the system's response). This paper will concentrate on the latter. In particular, we will present our inversion methodology which is based on minimizing the discrepancy between the simulated and measured normalized radar cross section data in the microwave regime. Through such an inversion technique, the complex permittivity profile of the domain of interest can be directly reconstructed by minimizing an appropriate data misfit cost function [4]. In addition, we can indirectly retrieve the profile's thermodynamics, geophysics, or inclusion properties [5, 6]. However, for such an inversion algorithm to be successful, some challenges exist at both data collection and processing levels, *e.g.*, collection of 'sufficient' amount of data (say, multi-view and/or multi-frequency) which is not trivial in sea ice remote sensing, and handling of the ill-posedness associated with the electromagnetic inverse scattering problem [7]. One can attempt to alleviate these issues by various means including the use of prior information, and appropriate regularization techniques [8].

This paper will investigate the possibility of oil detection in a sea ice environment. It should be noted that our focus is on the detection of spills rather than reservoirs (*e.g.*, see [9]). Previously, ground penetrating radar (*e.g.*, based on reflection-waveform inversion [10]), and SAR imagery (*e.g.*, based on polarization-ratio [11]) have been utilized for oil detection in ice-covered areas amongst other radar technologies [12, 13]. In this paper, we will introduce a physical-based retrieval model that utilizes radar cross section data. To this end, we initially present an overview on the general scheme of our inversion algorithm as applied to various snow-covered sea ice profiles (in the absence of oil spills) in Section 2. Next, we describe our oil-in-sea ice experiment, and present some collected data in Section 3. Herein, the primarily results are presented. In addition, it will be briefly discussed why our inversion strategy needs to be modified for this experiment. Further details pertaining this modified algorithm, and interpretation of the retrieved data will be explained in our presentation.

2 Electromagnetic Inversion

In the first part of our paper, we present an overview of our electromagnetic inversion algorithm developed for snow-covered sea ice remote sensing. Our inversion algorithm consists of an inverse solver and a forward solver. To find the parameters of interest, the inverse solver iteratively minimizes a cost function that is based on a discrepancy between the measured and the simulated electromagnetic response of the profile. To this end, we utilize the normalized

Figure 1. Bird's-eye view of the Sea-ice Environmental Research Facility (SERF) captured by drone. The circular oil in-sea-ice tank (pointed at by the vertical arrow) is located on the west side of the main SERF pool (pointed at by the horizontal arrow).

Figure 2. Normalized radar cross section (NRCS) measurements of the circular oil-in-sea ice tank through a C-band scatterometer. A trihedral calibration is performed in this scene.

radar cross section (NRCS) data as the measured input, defined as [14]

$$\sigma_{pq} \triangleq \frac{1}{A}\left\langle \lim_{R_r\to\infty}\left(4\pi R_r^2 \frac{S_s^p}{S_i^q}\right)\right\rangle \tag{1}$$

In (1), A is the surface area of the distributed target at an average distance of R_r in the farfield, S_i^q and S_s^p are the power densities of the incidence and scattered waves (q and p denote their respective polarizations). Also the symbol $\langle\,\rangle$ is defined as the ensemble average. Although the NRCS utilized in practical scenarios are usually collected through a SAR satellite [6], herein we concentrate on the NRCS data collected by an on-site scatterometer. This allows the collection of data in any desired angles or time from a selected profile within a small footprint, making it suitable for modeling and evaluation purposes. Regarding the cost function (denoted by CF), the general form utilized by the authors for our profile of interest is as follows

$$CF(\chi) \triangleq \sum_{m=1}^{M}\sum_{pq}\frac{\kappa}{\sigma_{pq}^{\text{meas}}(\psi_{\text{inc}}^m,\Psi_{\text{scat}}^m;f)}\times \left|\sigma_{pq}^{\text{meas}}(\psi_{\text{inc}}^m,\psi_{\text{scat}}^m;f) - \sigma_{pq}^{\text{sim}}(\chi;\psi_{\text{inc}}^m,\psi_{\text{scat}}^m;f)\right| \tag{2}$$

In (2), χ is the complex permittivity profile of interest, M is the number of the measurements, and pq denotes different polarizations utilized as *receive-send*. Moreover, ψ_{scat}^m and ψ_{inc}^m are the azimuth and elevation for the mth scattered and incidence angles respectively, at the frequency of f. Also in (2) for a unity κ, the weighting factor will normalize the difference in σ_{pq} to give equal weight to the data measured at different angles. It should be noted that if we have a prior knowledge of the sensitivity or uncertainty about the data, κ can be non-unity [4], or the data covariance matrix may be incorporated into the cost function [15]. Although a regularization-term seems to be absent in (2), we implicitly regularize our problem through a projection-based method. Finally, if a multi-frequency data set is available, an extra summation term over different frequencies of operation can be added to the above cost function.

We have previously utilized this scheme to retrieve various parameters of the snow-covered sea ice profile [4–6, 16] in the absence of oil. To this end, the profile is usually parametrized as a multi-layered rough medium with each layer being either homogenous (surface scattering) or having inclusions (volume scattering). To simulate the NRCS, the Boundary Perturbation Theory [17] in conjunction with our enhanced cloud-based volume scattering model have been implemented and previously utilized [6]. We have also demonstrated that Differential Evolution [18] as a global optimization scheme can find the global minimum of (2), if provided with enough data points and appropriate prior information. Finally, the thermodynamic and geophysical parameters of the profile can be retrieved through proxy formulae [14] that connect the profile's dielectric properties to its salinity, density, and temperature.

It should be noted that one of the main challenges with respect to parameter retrieval for these inversion methods is the lack of sufficient measured data. To tackle this, we have utilized various schemes previously. For instance, further parametrization of the profile based on our prior knowledge, use of more sensitive data with respect to the unknown to be retrieved, temporal inversion techniques, and addition of prior information from different platforms (*e.g.*, satellite imagery, lidar data) to the algorithm can alleviate the ill-posedness, and increase the retrieval accuracy [4–6].

3 Oil-Contaminated Sea Ice Experiment

The increased interest in Arctic shipping means a higher risk of spilling oil and similar contaminants into Arctic waters. Detection of such occurrences would be the first step in any clean-up scenario. In this section, we present our

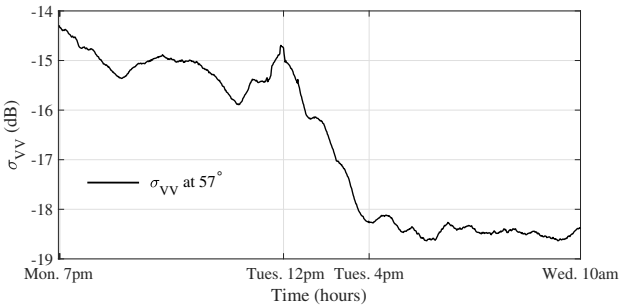

Figure 3. The calibrated measured vertically-sent vertically received NRCS (denoted by σ_{VV}) around the period of oil injection.

Figure 4. Oil-contaminated sea ice sampling.

measurements carried out in a controlled sea ice environment that is contaminated by crude oil. In this experiment, the oil was injected into the water column beneath the artificially grown sea ice while the profile's geophysical properties and NRCS response were measured temporally. The experiment was performed at the Sea-ice Environmental Research Facility (SERF) located at the University of Manitoba, from January to February of 2016. Figure 1 is a bird's-eye view from a drone looking down at SERF, and Figure 2 depicts the setting of our experiment. Since injection of crude oil to the main SERF pool, shown in Figure 1, would have resulted in cross-contamination with other ongoing projects, a specifically designed tank of 3 m diameter, shown at the west side of the main pool in this figure, was used in our experiment. A C-band scatterometer (shown in Figure 2) with a central frequency of 5.5 GHz was utilized to measure the polarimetric temporal NRCS. Figure 3 shows the calibrated measured NRCS before and after the oil injection for vertically-sent vertically-received polarization (denoted by σ_{VV}) at 57°. As can be seen in this figure, an NRCS drop of 3.3 dB is evident after the oil has settled in the profile. It should be noted that an external calibration through a metallic trihedral, and also a data calibration (with respect to a known sea ice profile) were performed on the raw NRCS data prior to use in our inversion algorithm.

There are a few challenges associated with the inversion problem regarding this experiment. First, due to the small size of the tank, only the NRCS data at one angle was considered reliable for inclusion in the inversion algorithm. Second, based on our on-site observation and later physical sampling, the actual distribution of the oil across the profile was heterogeneous. Therefore a multi-layer assumption for profile parametrization seemed unreasonable. Therefore, it was essential to consider a different inversion strategy than that outlined in Section 2. The details of the proposed inversion scheme will be explained in our presentation. In summary, the modified inversion scheme consists of an initial inversion of the pre-injection averaged NRCS data as well as a secondary inversion of the post-injection averaged NRCS data, assuming that the sea ice permittivity stays unchanged after injection. Moreover, we have used the data collected through a lidar system to provide surface roughness parameters as prior information to our inversion algorithm. Furthermore, we have assigned the boundaries of the search spaces for real and imaginary parts of the profile's complex permittivity based on our geophysical expectations (*i.e.*, use of projection-based regularization [8]).

An integral equation is used as our forward solver [14] working in conjunction with a Monte Carlo method for reconstructing the profile. This leads to the retrieval of an effective complex permittivity of $3.2 + 0.6i$ for the profile after oil injection. Using this reconstructed effective complex permittivity in conjunction with the reconstructed effective complex permittivity before oil injection, an effective oil volume fraction of 0.57 is obtained via the use of a dielectric mixing model. This can potentially trigger an oil spill alarm system when utilized in an integrated system as an auxiliary sensor alongside others.

It should be mentioned that based on the actual amount of the crude oil introduced, the retrieved value for the effective volume fraction is an over-estimation (roughly 7 times if the oil was uniformly distributed). We speculate that the following can explain this. (*i*) The oil has moved upward, and very close to the surface. Therefore considering the penetration depth of electromagnetic waves, a larger oil volume fraction with respect to the "visible" portion of sea ice will be observed by the interrogating waves. (*ii*) As opposed to the simplification utilized in our retrieval, the complex permittivity of the sea ice has not remained unchanged after the oil injection. To test the latter, physical sampling was performed as depicted in Figure 4. Based on the extracted samples, we further assessed our latter speculation through macro and micro approaches. As will be discussed during the presentation, the macro analysis shows a reduction of the bulk salinity and consequently, a reduction in sea ice permittivity. Moreover, to further investigate the oil distribution within the samples, a micro analysis utilizing *x*-ray scans, and chemical processing of the samples were performed. More details on our retrieved parameters and our follow-up analysis will be provided in our presentation.

4 Conclusion

We have performed an oil in young sea ice experiment to investigate the possibility of oil presence detection using C-band normalized cross section data. The physical sampling along with various observations in this experiment show that the oil distribution in the profile is heterogeneous, thus, making the use of a multi-layered model for profile parametrization challenging. Therefore, a modified retrieval algorithm was utilized to indirectly reconstruct the effective volume fraction of oil. This reconstructed value was an over-estimation. Based on macro-level (salinity measurements) and micro-level (x-ray scans) analysis, we noted two main reasons and speculations to explain this over-estimated reconstructed value, which will be further discussed in our presentation.

5 Acknowledgments

We acknowledge the financial contributions of the University of Manitoba's GETS program, Natural Sciences and Engineering Research Council of Canada, Canada Research Chair program, and Canada Excellence Research Chair program. This paper is also a contribution to the Arctic Science Partnership program and ArcticNet.

References

[1] T. Stocker, D. Qin, G. Plattner, M. Tignor, S. Allen, J. Boschung, A. Nauels, Y. Xia, V. Bex, and P. Midgley, *Climate Change 2013: The Physical Science Basis. Contribution of Working Group I to the Fifth Assessment Report of the Intergovernmental Panel on Climate Change*. Cambridge University Press, 2013.

[2] A. Jahn, J. E. Kay, M. M. Holland, and D. M. Hall, "How predictable is the timing of a summer ice-free Arctic?" *Geophysical Research Letters*, vol. 43, no. 17, pp. 9113–9120, 2016.

[3] L. Smith and S. Stephenson, "New Trans-Arctic shipping routes navigable by midcentury," *Proceedings of the National Academy of Sciences*, vol. 110, no. 13, pp. E1191–E1195, 2013.

[4] N. Firoozy, A. S. Komarov, J. Landy, D. G. Barber, P. Mojabi, and R. K. Scharien, "Inversion-based sensitivity analysis of snow-covered sea ice electromagnetic profiles," *IEEE J. Sel. Topics Appl. Earth Observ. in Remote Sens.*, vol. 8, no. 7, pp. 3643–3655, July 2015.

[5] N. Firoozy and et al., "Retrieval of young snow-covered sea-ice temperature and salinity evolution through radar cross-section inversion," *IEEE Journal of Oceanic Engineering*, vol. 41, no. 2, pp. 326–338, April 2016.

[6] N. Firoozy and et. al, "Landfast first-year snow-covered sea ice reconstruction via electromagnetic inversion," *IEEE Journal of Selected Topics in Applied Earth Observations and Remote Sensing*, vol. 9, no. 6, pp. 2414–2428, June 2016.

[7] V. Isakov, "Uniqueness and stability in multi-dimensional inverse problems," *Inverse Problems*, vol. 9, no. 6, p. 579, 1993.

[8] P. Mojabi and J. LoVetri, "Overview and classification of some regularization techniques for the Gauss-Newton inversion method applied to inverse scattering problems," *IEEE Trans. Antennas Propag.*, vol. 57, no. 9, pp. 2658–2665, 2009.

[9] A. Abubakar, T. M. Habashy, M. Li, and J. Liu, "Inversion algorithms for large-scale geophysical electromagnetic measurements," *Inverse Problems*, vol. 25, no. 12, p. 123012, 2009.

[10] J. H. Bradford, E. L. Babcock, H.-P. Marshall, and D. F. Dickins, "Targeted reflection-waveform inversion of experimental ground-penetrating radar data for quantification of oil spills under sea ice," *GEOPHYSICS*, vol. 81, no. 1, pp. WA59–WA70, 2016.

[11] C. Brekke, B. Holt, C. Jones, and S. Skrunes, "Discrimination of oil spills from newly formed sea ice by synthetic aperture radar," *Remote Sensing of Environment*, vol. 145, pp. 1 – 14, 2014.

[12] D. Dickins and J. Andersen, "Evaluation of airborne remote sensing systems for oil in ice detection," SINTEF Materials and Chemistry- Report no. 28, Tech. Rep., 2010.

[13] W. S. Pegau, J. Garron, and L. Zabilansky, "Detection of oil on-in-and-under ice - final report 5.3," Arctic Response Technology, Tech. Rep., 2016.

[14] F. T. Ulaby and D. G. Long, *Microwave Radar and Radiometric Remote Sensing*. University of Michigan Press, 2014.

[15] T. M. Habashy and A. Abubakar, "A general framework for constraint minimization for the inversion of electromagnetic measurements," *Progress in Electromagnetics Research*, vol. 46, pp. 265–312, 2004.

[16] P. Mojabi and et al., "Electromagnetic inversion for biomedical imaging, antenna characterization, and sea ice remote sensing applications," in *2016 URSI AP-RASC*, Aug 2016, pp. 586–589.

[17] P. Imperatore and et. al., "Electromagnetic wave scattering from layered structures with an arbitrary number of rough interfaces," *IEEE Trans. Geosci. Remote Sens*, vol. 47, no. 4, pp. 1056–1072, 2009.

[18] A. Qing, "Electromagnetic inverse scattering of multiple two-dimensional perfectly conducting objects by the differential evolution strategy," *IEEE Trans. Antennas Propag.*, vol. 51, no. 6, pp. 1251–1262, 2003.